JTTEE5 11:186-194

A Study of Processing Parameters in Thermal-Sprayed Alumina and Zircon Mixtures

Y. Li and K.A. Khor

(Submitted 10 July 1999; in revised form 14 December 2000)

A method of plasma spraying of alumina and zircon mixtures to form ZrO_2-mullite composites has been proposed and developed. The feedstock is prepared by a combination of mechanical alloying, which allows formation of fine-grained, homogeneous solid-solution mixtures, followed by plasma spheroidization that yields rapid solidified microstructures and enhanced compositional homogeneity. The effects of ball-milling duration and milling media were studied. It was found that zirconia is a more efficient milling media and that increasing milling duration enhanced the dissociation of zircon. Flame spray and plasma spray processes were used to spheroidize the spray-dried powders. The temperature of the flame spray was found to be insufficient to melt the powders completely. The processing parameters of the plasma spray played an important role in zircon decomposition and mullite formation. Increasing the arc current or reducing secondary gas pressure caused more zircon to decompose and more mullite to form after heat treatment at 1200 °C for 3 h. Dissociation of zircon and the amount of mullite formed can be enhanced significantly when using the more efficient, computerized plasma-spraying system and increasing the ball-milling duration from 4 to 8 h.

Keywords alumina, dissociation, plasma powder processing, plasma spheroidization, tetragonal zirconia, zircon

1. Introduction

Mullite ($3Al_2O_3 \cdot 2SiO_2$), the only stable compound in the alumina-silica system at room temperature and pressure, is well known for its creep resistance, high-temperature strength, chemical and thermal stability, and low thermal expansion.[1] In technical applications, the need for high purity, density, and homogeneity at reasonable sintering temperatures has prompted widespread interest in the processing of mullite. Many preparation methods for mullite from various chemical processes have been reported. In order to obtain high-purity and fine-grained mullite powders, various synthesis methods have been conducted, e.g., sol-gel method,[2,3] precipitation,[4,5] hydrolysis,[6,7] spray pyrolysis,[8-10] chemical vapor deposition,[11,12] etc. Although fine-grained and high-purity powder is required for a well-controlled microstructure of the fully densified bodies, the highly homogeneous distribution of the constituent elements in the starting powder is particularly important, especially in the case of multicomponent systems.[13] Two different formation routes have been found, i.e., direct mullitization from the amorphous state[14,15] at around 1000 °C and mullitization at higher temperatures, such as above 1200 °C by a spinel-type (a poorly crystalline high-alumina, $\sim 6Al_2O_3 \cdot SiO_2$, phase commonly referred to as "spinel") phase formation before mullitization.[16] However, this chemically synthesized mullite is costly and its productivity is very low.

Reaction sintering of Al_2O_3-zircon mixtures can be used to get ZrO_2-toughened mullite:

$$3Al_2O_3 + 2ZrSiO_4 \rightarrow 3Al_2O_3 \cdot 2SiO_2 + 2ZrO_2 \quad \text{(Eq 1)}$$

(if the mullite formed is of 3:2 stoichiometric composition). Various studies have been made to produce ZrO_2-mullite by reaction sintering.[17-20] However, mullitization normally requires relatively high temperatures and long duration because of the low bulk and grain-boundary diffusion coefficients for mullite. In order to reduce diffusion distances and to increase the driving force for sintering, preparation of mullite powders, which have fine particle size and homogeneity, is well recognized. This study starts from powder preparation to form ZrO_2-toughened mullite by mechanical alloying and thermal spraying.

Fine size, multicomponent ceramic powders may be prepared by directing a stream of high-velocity molten particles, produced by introducing powder into a thermal flame, into distilled water. Under certain conditions, the mixtures condense to form an aerosol, the droplets of which consist of a liquid-phase solution. The spheroidized powders are formed by rapid solidification of the individual droplets. The high cooling rate also tends to result in supersaturated solutions.[21] Quite different phases are produced at ambient temperatures than for sintered ceramics of the same composition. The structure of the final powders is then a function of the solidification processes, which occur within individual particles.[22]

The plasma-spray process is specified by the associated processing parameters where these influence the properties of the resultant deposits.[23,24] For a given particle, its velocity and temperature upon impact are linked on the one hand, to the plasma jet parameters—gas nature, velocity and temperature distributions, and turbulent mixing with the surrounding atmosphere—and on the other, to each particle trajectory in the plasma jet. The particle injection velocity, the position where it is inflected, its nature, density, size, and morphology control the trajectory.

Changing the processing parameters is the most common

Y. Li and **K.A. Khor,** School of Mechanical and Production Engineering, Nanyang Technological University, Singapore 639798, Singapore. Contact e-mail: mkakhor@ntu.edu.sg.

way of varying the properties of the deposits. The influence of spraying parameters is rather complex.[25] Of great importance are the power level and the kinds of plasma gases that are employed. The energy can be enhanced through the use of secondary gas. The purpose of the present article, therefore, was to examine how processing conditions affect particle melting by studying the influence of several process parameters on spheroidization of the powders. The present paper describes the preparation and processing of composite powders for use in thermal spraying by mixing high-purity zircon and alumina powders. By controlling the spheroidizing conditions, control of the final grain size and size distribution, as well as the dissociation of zircon, might be attained.

2. Experimental Techniques

Starting materials were high-purity $ZrSiO_4$ (99%) and Al_2O_3 (99.99%) powders obtained from Cerac, Inc. (Milwaukee, WI). Mixtures of $ZrSiO_4$ and Al_2O_3 powders with Al_2O_3:SiO_2 molar ratios of 3:2 were milled both with zirconia and alumina ball-milling media using the Fritsch P-5 Planetary Mill (WI, USA). The powder to ball ratio was kept to 1:10 by weight. The bowl was put on the mill and rotated at the speed of 200 rpm for different periods of time. The as-milled powders were spray dried with an LT-8 spray dryer (Ohkawara Kahohki Co., Ltd, Japan) to modify the particle shape of the ball-milled powders. Polyvinyl alcohol (PVA) was used as a binder. Subsequently, the spray-dried powders were heated in a furnace below 600 °C in order to burn off the PVA.

The composite powders after debinding and presintering were melted by (1) flame spraying with a Model FP-73 system (Miller Thermal, Inc., Appleton, WI), the combustion gas mixture was oxygen and acetylene; (2) plasma spraying with a 40 kW plasma torch SG-100 (Miller Thermal, Inc.); and (3) plasma spraying with a 100 kW computerized plasma-spraying system 4500 (Miller Thermal, Inc.). The Model 4500 plasma-spraying system uses sophisticated data-acquisition hardware and software to control, monitor, and record the plasma-spray processing functions through preprogrammed spray-parameter recipes, providing precise control of the complete plasma-spray process. The proprietary software programs include the ability to control and monitor the net plasma energy, which is the actual energy output in the plasma arc. Control of the net energy results in a proprietary parameter that allows the system to monitor the real-time gun efficiency. The plasma spraying guns use argon as primary gas and helium as auxiliary gas. The powders were heated in the hopper in order to prevent clogging along the passage towards the gun, then they were sprayed directly into water followed by collecting, drying, and sieving.

A Philips MPD 1880 diffractometer system (Philips Electronic Instruments Corp., Mahwah, NJ) was used for phase identification and crystallinity analysis of the powders. The relative phase ratios can be calculated by comparing the areas under peaks in the x-ray diffraction (XRD) pattern. Peak area under corresponding peak of different phases can be profile fitted using an automatic powder diffraction (APD) profile-fitting program. Phase ratios, R_{ZrO_2}, R_{ZrSiO_4}, and R_{mull}, were estimated by comparing the peak area of these phases:

$$R_{ZrO_2(m+t)} = \frac{I_{\{ZrO_2-t(111)\}} + I_{\{ZrO_2-m(11\bar{1})\}}}{I_{\{ZrSiO_4(200)\}} + I_{\{ZrO_2-t(111)\}} + I_{\{ZrO_2-m(11\bar{1})\}}} \times 100\% \quad \text{(Eq 2)}$$

$$R_{ZrSiO_4} = \frac{I_{\{ZrSiO_4(200)\}}}{I_{\{ZrSiO_4(200)\}} + I_{\{ZrO_2-t(111)\}} + I_{\{ZrO_2-m(11\bar{1})\}}} \times 100\% \quad \text{(Eq 3)}$$

$$R_{t-ZrO_2} = \frac{I_{\{ZrO_2-t(111)\}}}{I_{\{ZrO_2-t(111)\}} + I_{\{ZrO_2-m(111)\}} + I_{\{ZrO_2-m(11\bar{1})\}}} \times 100\% \quad \text{(Eq 4)}$$

$$R_{m-ZrO_2} = \frac{I_{\{ZrO_2-m(111)\}} + I_{\{ZrO_2-m(11\bar{1})\}}}{I_{\{ZrO_2-t(111)\}} + I_{\{ZrO_2-m(111)\}} + I_{\{ZrO_2-m(11\bar{1})\}}} \times 100\% \quad \text{(Eq 5)}$$

$$R_{mull} = \frac{I_{\{mull(210)\}}}{I_{\{ZrSiO_4(200)\}} + I_{\{Al_2O_3(012)\}} + I_{\{mull(210)\}}} \times 100\% \quad \text{(Eq 6)}$$

where $I_{Al_2O_3}$, I_{ZrSiO_4}, I_{t-ZrO_2}, I_{m-ZrO_2}, and I_{mull} are the integrated area intensities of the Al_2O_3, $ZrSiO_4$, t-ZrO_2, m-ZrO_2, and mullite corresponding peaks, respectively.

Microstructures were observed by scanning electron microscopy (SEM) equipped with electron dispersion. Differential thermal analysis (DTA) was carried out up to 1600 °C using a heating rate of 10 °C/min and a flowing nitrogen atmosphere (30 psi).

3. Results and Discussion

3.1 Mechanical Alloying

The average particle size of raw Al_2O_3 and $ZrSiO_4$ is 1.65 and 8.34 μm, respectively. The two kinds of powders were ball milled for different durations with different milling media (zirconia and alumina).

Mechanical alloying (MA) is a process for producing composite powders with a finely controlled microstructure. It can be used to modify alumina and zircon mixtures by refining the microstructure, homogenizing the composition, extending solubility, creating metastable crystalline phases, and even producing amorphous phases,[26] just as rapid solidification processes.

In this study, different milling media (alumina and zirconia) and different durations (4 to 20 h) have been selected to study the influence of MA on microstructure refining and composition homogeneity. The XRD results show that the intensities of the peaks corresponding to zircon decreased with the increasing milling duration, and our previous studies showed that the peaks for zircon disappeared after ~40 h of ball milling. Also, contamination from the milling media was detected by XRD if the milling duration was longer than 8 h in the zirconia medium and 3 h in the alumina medium. The ball-milled powders were then spray dried and plasma spheroidized. It is anticipated that the MA effect on the phase composition of the powder mixture could be better elucidated after spheroidization.

3.2 Spray Drying

The flow characteristic of powders is dependent on the particle size, particle size distribution, and particle morphology.

Table 1 Parameters Used to Prepare $Al_2O_3 + ZrSiO_4$ Powder Using the Spray-Drying Technique

Process Part	Parameters
Slurry composition in wt.%	75% water, 24% ($Al_2O_3 + ZrSiO_4$), 1% PVA
Atomization technique	Rotating disc, rotation speed 30,000 rpm
Droplet air mixing	Air inlet temperature 240 °C Air outlet temperature 140 °C

Finer particles with wider size distribution and irregular shape often have difficulty flowing consistently. Also, rough particle surface obviously would reduce the flowability of particles. Spray drying consists of transforming a suspension/fluid into a granular solid by dispersion in a drying medium. The products manufactured using this technique are well adapted to thermal spraying because of the following properties:

- the size and granulometric distribution are easily controllable,
- good flowability,
- suitable morphology, and
- homogeneous chemical composition.

In this study, water content and rotation speed of the atomizer were varied from 70 to 85 wt.% and 10,000 to 30,000 rpm, respectively. It was found that the composition of the slurry and the atomization speed play an important role in controlling the particle morphology and particle size distribution of the spray-dried powders. The lower water content and the lower rotation speed of the atomizer led the particle distribution to a larger particle size range. The typical spray-drying parameters used for $Al_2O_3 + ZrSiO_4$ powder preparation are given in Table 1.

Particle morphology and particle size distribution of spray-dried composites of alumina and zircon are shown in Fig. 1. There is no phase change during spray drying. Most of the particles are almost spherical. The flowability of this powder was superior to that of the ball-milled powder. Under high magnification, it was found that small particles are agglomerated together to form aggregates. Some of the particles have micropores. It may be thought that considerable evaporation occurs during the first few milliseconds of drying. Rapid heating may cause liquids to evaporate within the droplet, forming a bubble-like effect that may expand the agglomerate. When the bubble breaks through the skin and collapses and the agglomerate is depressed, a dimpled or donut shape is formed.[27]

The agglomerated particles may partially "explode" upon penetration into the plasma jet.[28] This is probably due to their poor mechanical resistance and the high thermal shock experienced when the gas is trapped in the pore structure and the particles rapidly expend on exposure to the plasma jet. The exploded particles do not penetrate into the jet because their momentum is too low; thus, they travel in its periphery and are dragged into the jet due to the large vortices created at the jet fringes. This results in a much lower velocity and surface temperature. Thus, in this study, the spray-dried powders were debinding below 600 °C followed by presintering at 1000 °C for 2 h in order to form solidified powders.

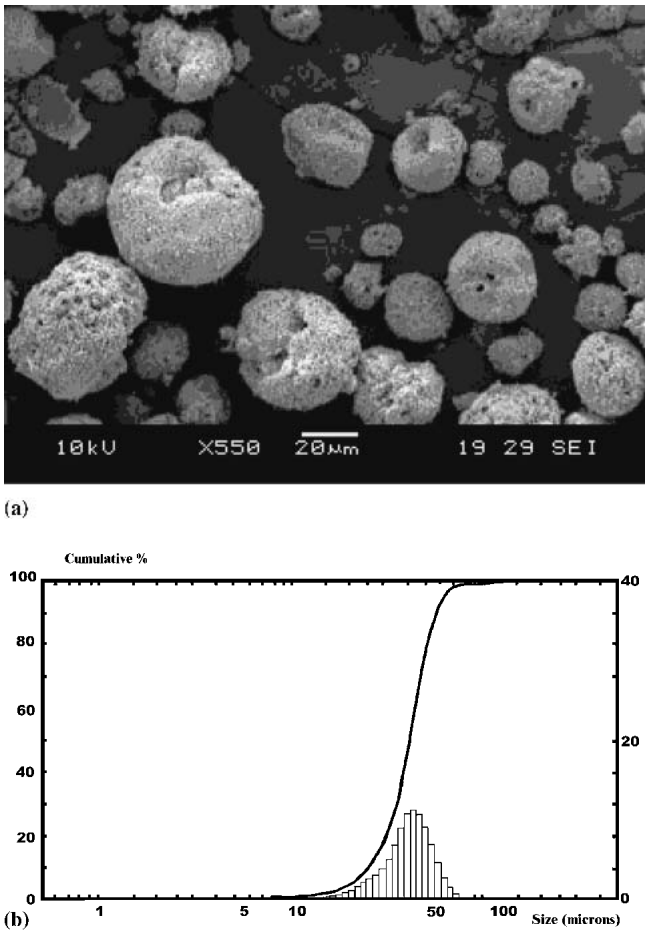

Fig. 1 **(a)** The SEM micrograph and **(b)** particle size distribution of spray-dried composite powders of alumina and zircon

3.3 Spray Spheroidization

The spray-dried powders with different ball-milling duration were spheroidized by three kinds of methods, i.e., combustion flame spray, 40 kW plasma spray that was operated manually, and computerized 100 kW plasma spray by a robotic system. For a given combustion flame (nozzle diameter, power level, gas nature, and flow rate), the momentum of the injected particles has to be adapted to that of the flame jet so that they travel in the hot zones of the jet. For any given flame type, carrier gas, gas injector, and powder size distribution, vastly differing mean droplet trajectories can be observed depending on the carrier-gas flow rate. If the flow rate is low, the particles do not penetrate into the jet plume, and if it is excessively high, they pass through it completely. The optimum trajectory that corresponded to the highest surface temperature resulting in the highest deposition efficiency was obtained by adjusting the carrier-gas flow rate.

Flame Spray. The powders ball milled for 4 h with zirconia balls and bowl, followed by spray drying, were used to spheroidize by combustion flame spraying. From the XRD diffraction spectra (Fig. 2), it was found that the peaks corresponding to zircon are still the main ones, although t-ZrO_2 formed after

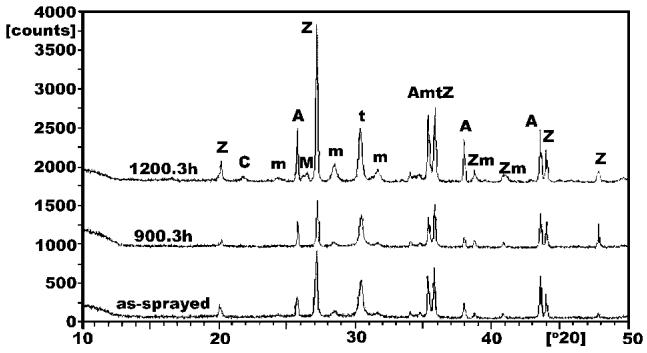

Fig. 2 The XRD diffraction spectra of the flame spheroidized powders followed by heat treatment at 900 and 1200 °C for 3 h (M: mullite, A: alumina, Z: zircon, t: t-ZrO_2, m: m-ZrO_2, and C: cristobalite)

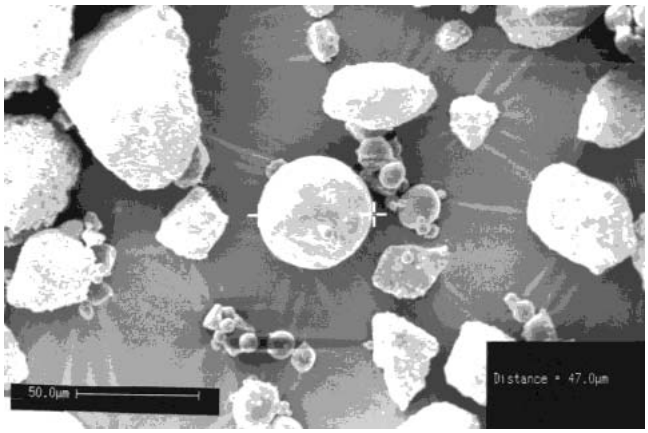

Fig. 3 The SEM micrograph of the flame spheroidized powders

flame spray, revealing that zircon did not decompose significantly due to the relative low temperature of the combustion flame (~2600 °C). After heating at 1200 °C for 3 h, mullite formed, but the amount of mullite was lower, and intensities of the peaks corresponding to zircon were much higher relative to those of ZrO_2 at 900 °C, indicating that zircon recombined.

Under SEM, it is clear that only the small particles have been spheroidized, the largest diameter of the fully melted powders is about ~45 μm, and many particles have irregular shape, as shown in Fig. 3. These results indicate that flame spray cannot melt the powders well.

Plasma Spheroidization with the 40 kW Plasma Spray System (SG-100). The powders used to plasma spheroidize with a manual gun were the same as in flame spraying. The power level was changed by adjusting the plasma arc current at 600, 800, and 1000 A (Ar: 50 psi, and He: 40 psi). Some powders were plasma sprayed into water with the secondary gas pressure at 40, 20, and 0 psi, respectively (current: 800 A). After collecting, drying, and sieving, the spheroidized powders were used to study particle morphology, size distribution, and phase identification.

It was found that when the arc current is 600 A, most of the spherical particles are less than 20 μm, while the larger ones remained as partially molten. When sprayed at 800 A, the composite powders became denser, approaching spherical shape, and had smooth surfaces. The flowability is much better than that of powders after spray drying. Ultrafine powders agglomerate to form aggregates when the current is at 1000 A. Powders with similar morphology to that sprayed at 1000 A current were obtained when the secondary gas pressure was decreased to 20 and 0 psi.

The DTA curve of spheroidized powders shows that there is an exothermic peak at 1012 °C. The XRD patterns of the spheroidized powders that were heated at 900 and 1200 °C for 3 h indicated that the exothermic peak is attributed to the formation of mullite.[29]

Figure 4 shows the effects of power level and secondary gas pressure on the dissociation of zircon and formation of mullite in the plasma-sprayed powders. Mullite formed after heat treating the plasma-sprayed powders at 1200 °C for 3 h. It could be seen that the relative phase ratio of zircon decreased with increasing

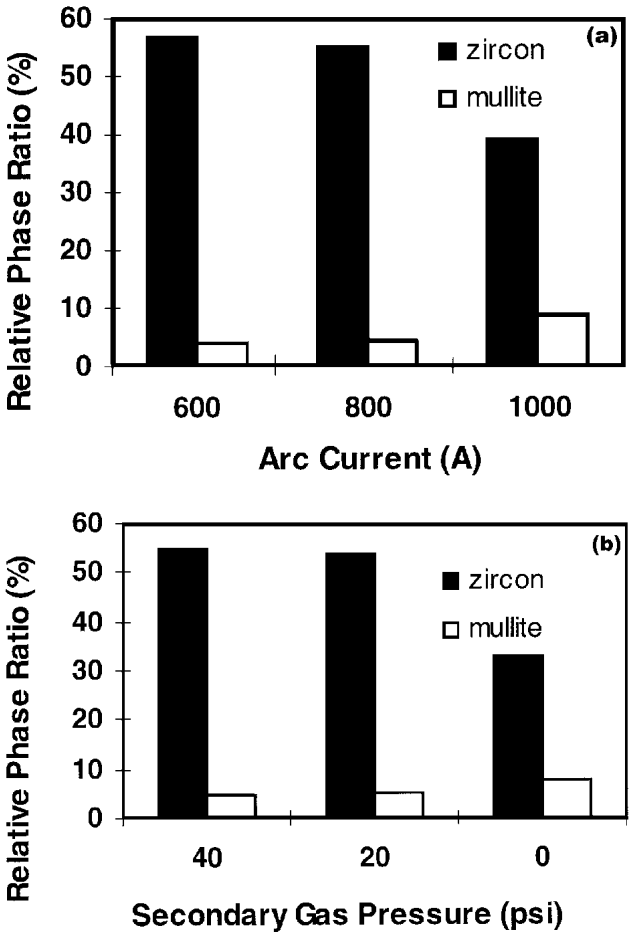

Fig. 4 Effects of **(a)** power level and **(b)** secondary gas pressure on the dissociation of zircon and formation of mullite in the plasma-sprayed powders

the current from 600 to 1000 A, indicating that more zircon dissociated or became amorphous. In the melting process, the starting powder may change from crystalline to an amorphous phase; while in the resolidification process, the amorphous phase be-

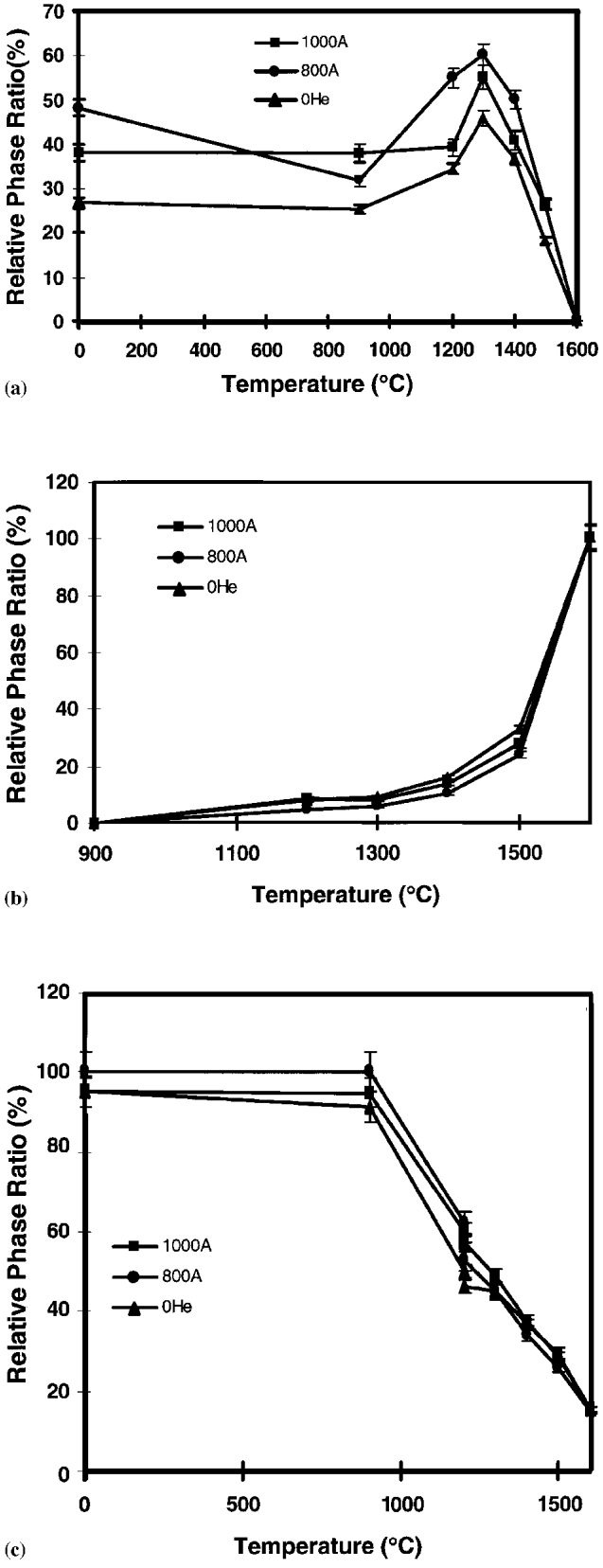

Fig. 5 Relative phase ration of **(a)** zircon, **(b)** mullite, and **(c)** t-ZrO_2 vs temperature in the spheroidized powders

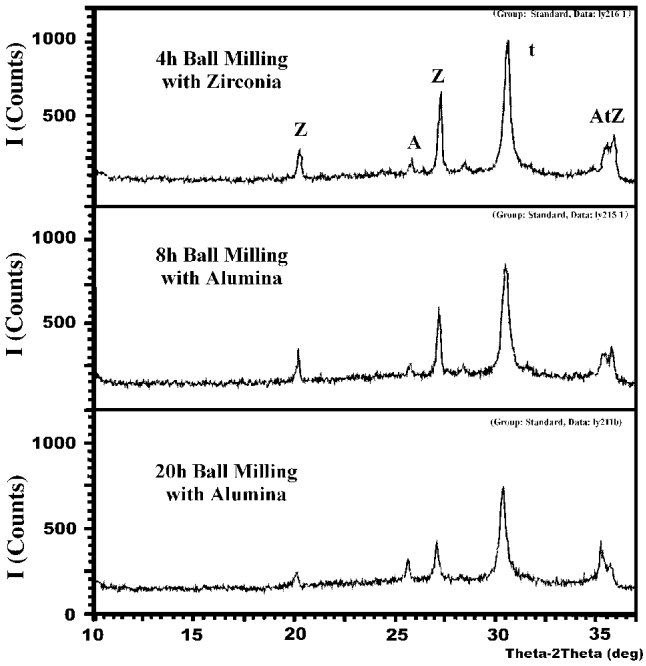

Fig. 6 The XRD patters of the spheroidized powders ball milled with different milling media and for different milling duration (A: alumina, Z: zircon, and t: t-ZrO_2)

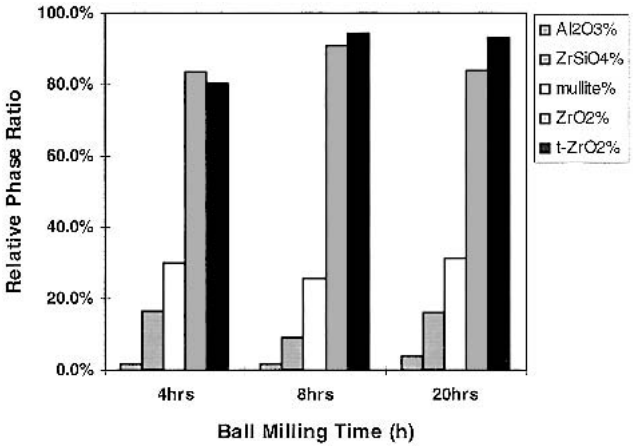

Fig. 7 Effects of ball-milling time and media on mullitization of the spheroidized powders (1200 °C and 3 h)

gins to recrystallize.[30] The amount of mullite increased when the arc current was increased. However, increasing the power level, on one hand, should increase the velocity of the plasma jet. Any increase in the plasma jet velocity enhances thermofluid interaction with the surrounding atmosphere[31] (known as pumping), which, when it is air, rapidly cools the plasma jet and reduces its length and diameter.[32] On the other hand, the enthalpy of the flame increased more significantly with increasing current, causing more zircon to be dissociated or to become amorphous; alumina and silica from the dissociated zircon formed a solid solution with a series solubility.[33] All these promote mullite formation. When increasing the secondary gas

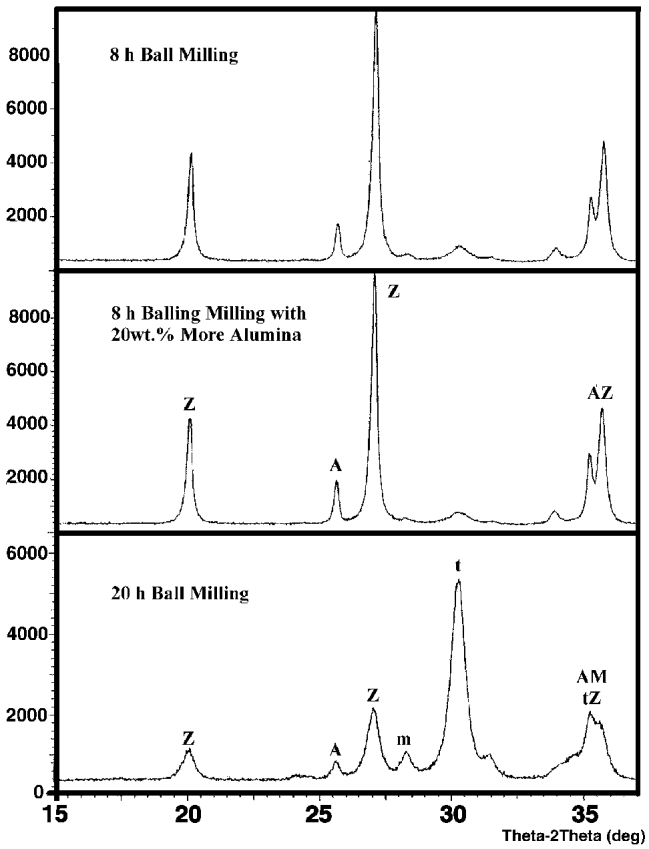

Fig. 8 The XRD patterns for the powders ball milled for different duration with zirconia milling media followed by solidification at 1000 °C for 2 h (A: alumina, Z: zircon, t: t-ZrO_2, and m: m-ZrO_2)

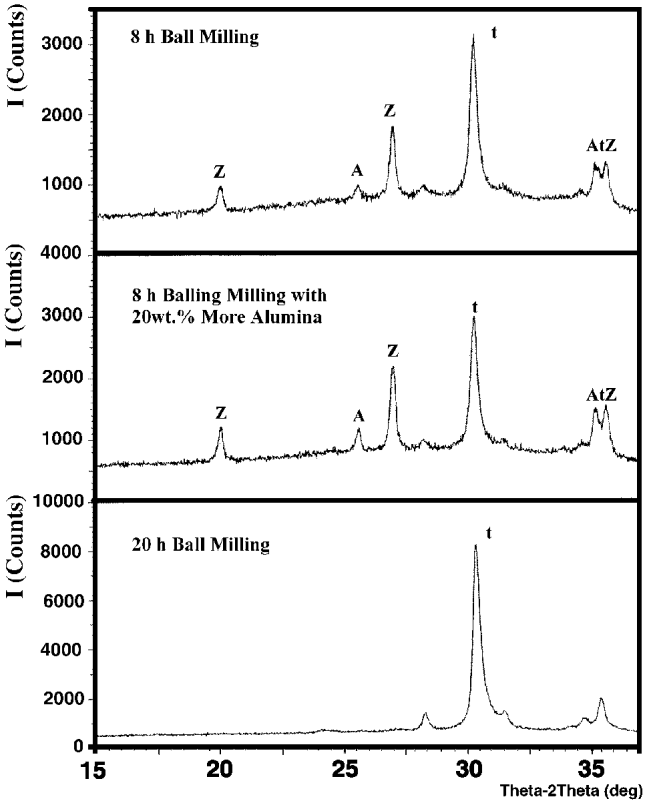

Fig. 9 The XRD patterns of the spheroidized powders ball milled for different duration with zirconia milling medium (A: alumina, Z: zircon, and t: t- ZrO_2)

(He) pressure from 0 to 20 and 40 psi, the enthalpy and the thermal conductivity of the plasma gas should be enhanced. However, the velocity of the plasma gas increased with increased flow rate, which resulted in a shorter residence time. Thus, the relative phase ratio of zircon increased with increasing the secondary gas pressure from 0 to 40 psi, indicating that less zircon dissociated. The amount of mullite decreased when the secondary gas pressure increased, as shown in Fig. 4(b).

Figure 5 shows the relative phase ratio of zircon, mullite, and t-ZrO_2 in the spheroidized powders after heat treatment at different temperatures. There is a temperature range (1200-1400 °C) at which the dissociated zircon recombined during spheroidization. When heated above 1400 °C, zircon decomposes fast. The amount of mullite remains low below 1300 °C and increases significantly at higher temperatures. Most of the t-ZrO_2 is relatively stable below 1000 °C.

Spheroidization with the 100 kW Computerized Plasma Spraying System. Optimized spray distance and power levels were selected by comparing the crystallinity and microstructure of the powders. It was found that 12 cm spray distance and net energy at 14 to 15 kW is the best condition to melt the composite powders.

Figure 6 shows the XRD patterns of the spheroidized powder ball milled with zirconia for 4 h, and with alumina for 8 and 20 h. The relative phase ratio of zirconia is almost the same in the three kinds of powders, which means that the dissociation of zircon remained almost at the same level. The relative phase ratio of alumina increased with increasing ball-milling time when alumina was used as a milling media. This may be caused by contamination during ball milling. It was found (Fig. 7) that there was an insignificant difference in the amount of mullite after 3 h heat treatment at 1200 °C. The amount of mullite in the powder ball milled for 4 h with zirconia media and the powder ball milled for 20 h with alumina media is virtually similar, while the powder ball milled for 8 h with alumina media has the least amount of mullite. These results indicate that the effect of ball milling in alumina is not significant even after a 20 h milling duration compared with that of zirconia milling media.

Effects of zirconia milling media are shown in Fig. 8. We also increased the composition of alumina by 20 wt.% in one sample in order to study the composition influence. It could be seen that zircon dissociates much more after 20 h ball milling than after 8 h milling. After spheroidization, zircon completely dissociated in the sample of 20 h ball milling, as shown in Fig. 9. These indicate that the ball-milling effect of zirconia is more evident than that of alumina. However, there is more contamination from the milling media after 20 h milling (Fig. 8), while contamination cannot be detected by XRD after 8 h ball milling with zirconia media. It was also found that an increase of alumina in the composite could not increase the amount of mullite. This is in agreement with the results of other workers, showing that

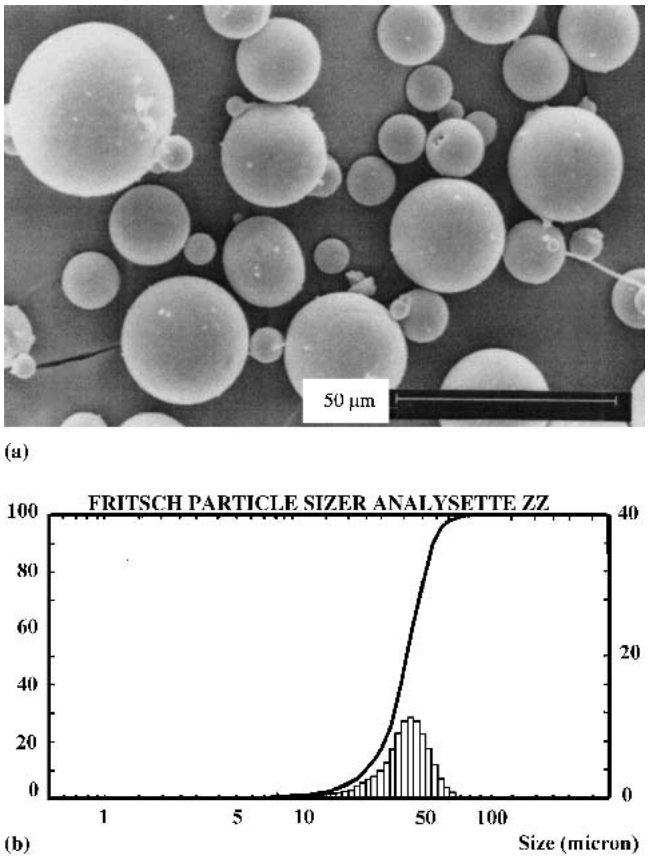

Fig. 10 Morphology of the spheroidized powder and its particle size distribution

mullitization mechanisms in mixtures of various polymorphs of Al_2O_3 and SiO_2 are greatly influenced by the properties of the reactants and less by the bulk chemical composition.[34] In order to control the contamination and study the dissociation of zircon and mullitization, we simply select 8 h ball milling with zirconia milling media. Morphology of the spheroidized powder and its particle size distribution is given in Fig. 10.

The influence of ball milling time and media can be explained as follows. The atomically mixed alumina and silica species, present at the interface between alumina-rich inhomogeneities and the silica-rich amorphous matrix, undergoes a rapid transformation after ~980 °C, and this transformation causes a rearrangement at the interface. The result of this transformation is alumina-rich mullite at the interface, while within the inhomogeneities this transformation catalyzes the crystallization of spinel.[33] The size of the inhomogeneities determines the major crystalline phase. As the inhomogeneities decrease in volume with the increasing ball-milling time and efficient milling media, the relative importance of the interface increases, and the amount of mullite yielded on completion of the exotherm increases.

Figure 11 compares the three kinds of spheroidization methods. It can be seen that the dissociation of zircon and the amount of mullite can be enhanced significantly when using the more energy efficient computerized 100 kW plasma spraying system and increasing the ball milling duration from 4 to 8 h. The

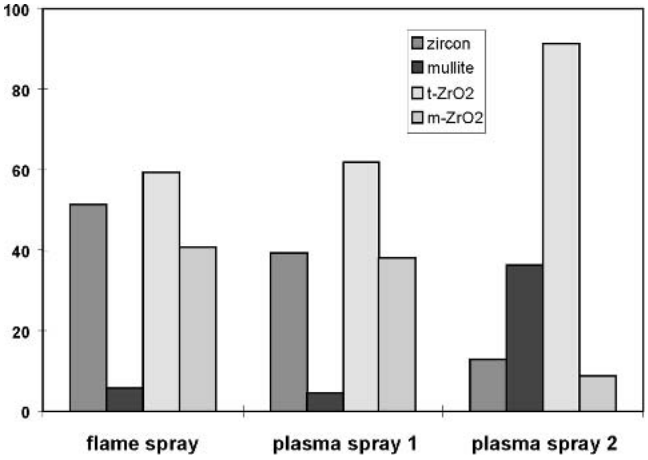

Fig. 11 Effects of different spheroidization methods on dissociation of zircon and mullite formation (plasma spray 1 = 40 kW plasma spray, manual control, and plasma spray 2 = 100 kW robotic control)

amount of mullite increased about sixfold, and more than 90% zirconia remained in the tetragonal phase, as compared with only ~60% tetragonal zirconia after spheroidization using combustion flame spray and the 40 kW plasma spray gun. The relative phase ratio of undissociated zircon after spheroidization using flame spray, 40 kW plasma spraying, and 100 kW plasma spraying system is 51.3, 39.1, and 13%, respectively.

Finally, Fig. 12 illustrates the difference observed among the powders spheroidized by the 40 kW plasma torch and the 100kW computerised plasma spray system. The polished cross-section of the powders spheroidized by the 40 kW plasma torch (Fig. 12a,b) demonstrates evidence of incomplete melting of the feedstock in the plasma flame. Remnants of the original zircon are observed in the powders. Conversely, the polished cross section of the powder spheroidized in the 100kW computerised plasma spray system (Fig. 12c) shows complete melting. Further evidence is observed in the EDS spectrum (Fig. 12d) that confirmed that the melted powder revealed the presence of the elements Al, Si, Zr and O. Thus, validating that the original content of the feedstock was preserved through the spheroidization process.

Conclusions

A method of fabricating ZrO_2-mullite composites based on plasma spraying of alumina and zircon mixtures has been proposed and developed ($3Al_2O_3 + 2ZrSiO_4 = 2Al_2O_3 \cdot 2SiO_2 + 2ZrO_2$). The feedstock is prepared by a combination of mechanical alloying (MA), which allows formation of fine-grained, homogeneous solid-solution mixtures, and plasma spheroidization that yields rapid solidified microstructures and enhanced compositional homogeneity. The effects of ball-milling duration and milling media were studied. It was found that zirconia is a more efficient milling media and increasing milling duration enhanced dissociation of zircon. Zircon disappeared in the spheroidized powders after 20 h ball milling with zirconia milling media. Three kinds of methods were used to spheroidize the spray-dried powders. The temperature of the flame spray is not

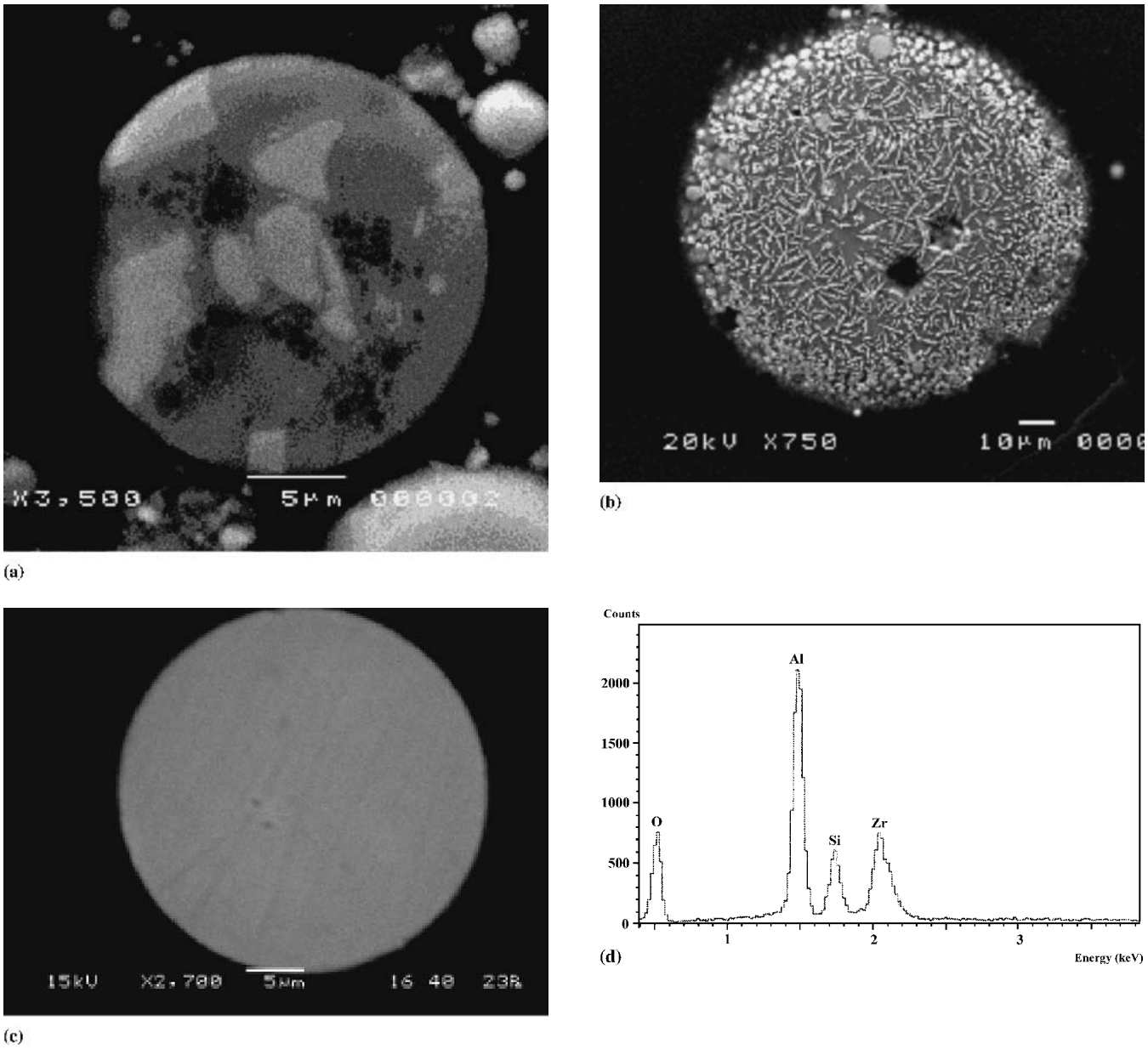

Fig. 12 Backscattered electron image on the spheroidized powders: **(a)** and **(b)** cross section of powders spheroidized by the 40 kW plasma torch; **(c)** cross section of powders spheroidized by the 100 kW computerized plasma-spraying system; and **(d)** the EDS spectrum of (c)

high enough to melt the powders completely. The processing parameters of plasma spray played an important role in zircon decomposition and mullite formation. Increasing the arc current or reducing the secondary gas pressure caused more zircon to dissociate. Consequently, more mullite formed after heat treatment at 1200 °C. Dissociation of zircon and the amount of mullite can be enhanced significantly when using the more efficient, robotic plasma-spraying system and increasing the ball-milling duration from 4 to 8 h. The amount of mullite increased about sixfold, and more than 90% zirconia remained as tetragonal comparing with only ~60% tetragonal zirconia after spheroidization using flame spray and the 40 kW plasma spray gun. The relative phase ratio of undissociated zircon after spheroidization using flame spray, 40 kW plasma spraying, and 100 kW plasma spraying system is 51.3, 39.1, and 13%, respectively.

References

1. I.A. Aksay, D.M. Dabbs, and M. Sarikaya: *J. Am. Ceramic. Soc.*, 1991, *74*(10), pp. 2343-57.
2. H. Schneider, M.G.M.U. Ismail, and K. Katayama: *J. Eur. Ceram. Soc.* 1993, *11,* pp. 87-94.
3. K. Nishu, T. Yokoyama, T. Watanabe, and T. Tarutani: *Abstract of the 27th Symp. on the Basic Science of Ceramics*, Ceramic Society of Japan, Tokyo, 1989, paper no. 1B08.
4. J. Okada and N. Otsuka: *J. Am. Ceram. Soc.,* 1986, *69*(9), pp. 652-56.
5. H. Yamada and S. Kimura: *Yogyo-Kyokaishi*, 1962, *70,* pp. 87-93.

6. Y. Hirata, K. Sakeda, Y. Matsushita, K. Shimada, and Y. Ishihara: *J. Am. Ceram. Soc.*, 1989, *72,* pp. 995-1002.
7. K. Okada, Y. Hoshi, and N. Otsuka: *J. Mater. Sci. Lett.,* 1986, *5,* pp. 1315-18.
8. S. Kanzaki, H. Tabata, T. Kumazawa, and S. Ohta: *J. Am. Ceram. Soc.*, 1985, *68,* pp. C6-C7.
9. K. Hamano, Z. Nakagawa, G. Cun, and T. Sato: in *Mullite*, S. Somiya, ed., Uchida Rokakuho Publishing, Tokyo, 1985, pp. 37-49.
10. O. Sakurai, N. Mizutani, and M. Kato: *J. Ceram. Soc. Jpn.*, 1988, *96,* pp. 639-45.
11. S. Hori and R. Kurita: *Ceram. Trans.* 1990, *6,* pp. 311-22.
12. S.L. Chung, Y.C. Sheu, and M.S. Tsai: *J. Am. Ceram. Soc.*, 1992, *75,* pp. 117-23.
13. S.K. Tabata and T. Kumazawa: *Ceram. Trans.*, 1990, *6,* pp. 339-51.
14. J. Ossaka: *Nature (London)*, 1960, *19*(4792), pp. 1000-01.
15. D.W. Hoffman, R. Roy, and S. Komarneni: *J. Am. Ceram. Soc.*, 1984, *67,* pp. 468-71.
16. J. Okada and N. Otsuka: *J. Am Ceram. Soc.*, 1986, *69*(9), pp. 652-56.
17. E. Di Rupo, T.G. Carruthers, and R.J. Brook: *J. Am. Ceram. Soc.*, 1978, *61,* p. 468.
18. E. Di Rupo and M.R. Anseau: *J. Mater. Sci.*, 1980, *15,* p. 114.
19. N. Claussen and J. Jahn: *J. Am. Ceram. Soc.*, 1980, *63,* pp. 228-29.
20. J.S. Wallace, G. Petzow, and N. Claussen: *Adv. Ceram*., 1984, *12,* pp. 436-42.
21. G.N. Heintze and R. McPherson: in *Advances in Ceramics, 24: Science and Technology of Zirconia III,* Am. Ceram. Soc., Westerville, OH, 1988, *24,* pp. 431-37.
22. R. McPherson: *Proc. Int. Round Table on Study and Application of Transport Phenomena in Thermal Plasma*, Odeillo, France, 1975, IUPAC/CNRS IV, pp. 8-14.
23. I.A. Fisher: *Int. Metall. Rev.*, 1972, *17,* pp. 117-29.
24. J. Ilavsky, A.J. Allen, G.G. Long, and S. Krueger: *J. Am. Ceram. Soc.*, 1997, *80*(3), pp. 733-42.
25. P. Fauchais, J.F. Coudert, A. Vardelle, M. Vardelle, and A. Denoirjean: *J. Thermal Spray Technol.,* 1992, *1*(2), pp. 117-28.
26. K.A. Khor and Y. Li: *Mater. Sci. and Eng.*, 1998, *A256,* pp. 271-79.
27. J.S. Reed: *Introduction to the Principles of Ceramic Processing*, Wiley and Sons, New York, NY, 1995.
28. M. Vardelle, A. Vardelle, and P. Fauchais: *J. Therm. Spray Technol.*, 1993, *2*(1), pp. 79-86.
29. Y. Li and K.A. Khor: *Int. Thermal Spray Conf. '98 (ITSC'98)*, C. Coddet, ed., ASM International, Metals Park, OH, 1998, pp. 1233-38.
30. K.A. Gross and C.C. Berndt: in *Bioceramics*, J. Wilson, L.L. Hench, and D. Greenspan, ed., Pergamon Press, Oxford, United Kingdon, 1995, pp. 215-368.
31. R. Spores and E. Pferder: *Surf. Coat. Technol.*, 1989, *37,* pp. 251-60.
32. P.H. Roumilhac, J.F. Coudert, and P. Fauchais: *Materials Research Society Symposia Proceedings*, MRS, Pittsburgh, PA, 1991, *190,* p. 227.
33. Y. Li and K.A. Khor: unpublished research.
34. F.M. Wahl, R.E. Grimm, and R.B. Graf: *Am. Min.*, 1961, *46,* pp. 1064-76.